THE JOURNAL OF PHYSICAL CHEMISTRY B

Article

pubs.acs.org/JPCB

Guest-Induced Crystal-to-Crystal Transitions of Poly(L-lactide) Complexes

Hironori Marubayashi,[†,‡] Shigeo Asai,*[,†] and Masao Sumita[†]

[†]Department of Chemistry and Materials Science, Graduate School of Science and Engineering, Tokyo Institute of Technology, Ookayama, Meguro-ku, Tokyo 152-8552, Japan

Supporting Information

ABSTRACT: In this study, we systematically investigated various crystal-to-crystal transitions relating to poly(L-lactide) (PLLA) cocrystallized with low-molecular-weight compounds using wide-angle X-ray diffraction and Fourier transform infrared spectroscopy. First, the solvent exchange and the resultant crystal transition of solvent complexes were investigated. Basically, the solvent exchange treatments at −25 °C became successful, although some specific phenomena depending on solvent species were seen. The ratio of the α-form in the crystalline region increased by an increase in the solvent exchange temperature. Second, the crystal transition behavior between CO_2 and solvent complexes was investigated. The complete transition from solvent complex to CO_2 complex was observed for all solvent complexes. In contrast, it was found that types of solvents and the surrounding temperature have a great effect on the transition behavior from CO_2 to solvent complexes. Finally, the guest-induced transitions of noncomplex crystals (α-, α′-, and α″-forms) were examined. As a result, it was revealed that the guest-induced transition behavior of noncomplex crystals was much influenced by the order of crystal (chain conformation and packing) of noncomplexes (α, α′, and α″) as well as kinds of guests.

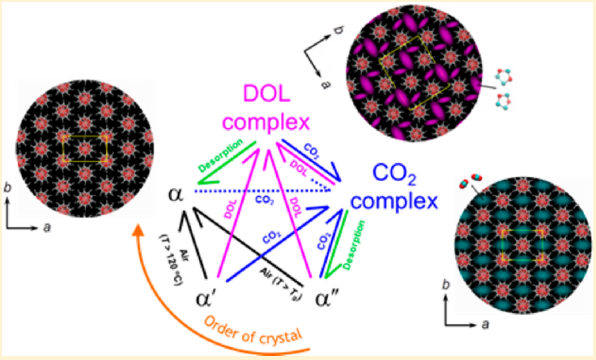

INTRODUCTION

Poly(L-lactide) (PLLA), whose chemical structure is −[−OCH(CH$_3$)CO−]$_n$−, is one of the biobased polymers expected to be alternatives to petroleum-based polymers.[1] It is well-known that PLLA forms several types of crystal structures (crystal polymorphism) depending on surrounding conditions: α-form,[2,3] α′ (δ)-form,[4,5] α″-form,[6] β-form,[7] and γ-form.[8] Furthermore, PLLA forms cocrystals with specific low-molecular-weight compounds under specific conditions: CO_2 complex[6] and solvent complexes (ε-forms),[9] as shown in Figure 1. Roughly speaking, PLLA chains take the 10/7 (left-handed 10/3) helical conformation in the α, α′, CO_2 complex, and solvent complexes, whereas they take the 3/2 (left-handed 3/1) helical conformation in the β- and γ-forms. For the PLLA crystals with 10/7 helices (α, α′, and ε), it was reported that PLLA chains are distorted from the ideal 10/7 helix.[3,5,9] Compared with the α-form, the oriented CO_2 complex film showed shorter *a*-axis, longer *b*-axis, and shorter *c*-axis lengths, resulting in a slight increase in the unit cell volume.[6b] It was indicated that the chain helical conformation of PLLA in the CO_2 complex is similar to but different from that in the α-form (10/7 helix for both forms), because of the interaction between PLLA and CO_2.[6b] It seems likely that CO_2 molecules are encapsulated in the cavity surrounded by four PLLA chains.[6b] Marubayashi et al. reported that PLLA chains in the ε-form take the 10/7 helical conformation and are packed in the orthorhombic unit cell (*a* = 1.5−1.6 nm, *b* = 1.2−1.3 nm, and *c* = 2.8−2.9 nm).[9] For the PLLA−*N*,*N*-dimethylformamide (DMF) complex (one of the PLLA−solvent complexes), it was proposed that four PLLA chains and eight DMF molecules are packed in the unit cell.[9]

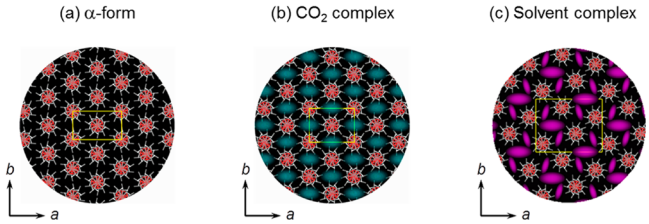

Figure 1. Comparison of *ab* planes of (a) PLLA α-form (*a* = 1.068 nm, *b* = 0.617 nm, and *c* (fiber axis) = 2.886 nm; orthorhombic[3b]), (b) PLLA−CO_2 complex (*a* = 0.96 nm, *b* = 0.73 nm, and *c* (fiber axis) = 2.86 nm; orthorhombic[6b]), and (c) PLLA−solvent complex (ε_{DMF}-form, *a* = 1.551 nm, *b* = 1.227 nm, and *c* (fiber axis) = 2.857 nm; orthorhombic[9]). The unit cell is shown by a yellow rectangle. Guest positions are schematically represented by ellipsoids. Helix distortion from the ideal 10/7 helix is not considered here for simplicity. Hydrogen atoms in methyl groups of PLLA are omitted.

Studies on crystal transitions are of great importance in the use of a material. If the crystal structure is changed by the

Received: September 10, 2012
Revised: December 6, 2012
Published: December 6, 2012

surrounding atmosphere, there will be changes in its material properties in varying degrees. Syndiotactic polystyrene (sPS) shows crystal polymorphism and a complicated crystal transition behavior containing several cocrystals with solvent molecules.[10] Hashida et al. investigated the water-induced phase transition of polyethylenimine (PEI) from molecular, crystal, and higher-order levels by simultaneous measurements of wide-angle X-ray diffraction (WAXD), small-angle X-ray scattering (SAXS), and Raman spectra.[11] The crystal transition behavior of PLLA is mentioned here. When a tensile force is applied to the α-form, the breakage of the large domain into smaller domains as well as conformational disordering occurs, resulting in the appearance of the α'-form.[5a] Further stretching transforms the α'-form (disordered 10/7 helix) into the β-form (3/2 helix).[5a] The crystal transition from α'-form to α-form has been studied extensively by many reseachers.[4,5] In the cold crystallization process of PLLA, small domains of the mesophase grow larger to form the domains of the α'-form, attendant with the imperfect conformational regularization as well as the disorder in relative height between the neighboring domains.[5b] By increasing the temperature further, the α'-form transforms to the α-form consisting of more tightly packed chains of regular conformation in the domain with a larger size.[5b] Marubayashi et al. reported that CO_2 desorption from the PLLA−CO_2 complex film induces the transition to the α'' (draw ratio $\leq$2) or α (draw ratio >2).[6b] They also revealed that the ε-to-α transition occurs with solvent desorption, in which solvent solubility of 0.3−0.4 g/g_{PLLA} is a starting point.[9] Lai et al. revealed that the addition of 1,3:2,4-dibenzylidene-D-sorbitol (DBS) changes the crystal structure and the crystallization rate of PLLA.[12]

There are specific crystal polymorphs that need multistep crystallization treatments. In the cases of sPS−solvent cocrystals, the formation of specific crystal structures arises by solvent desorption (γ,[13] δ,[14] and ε[15]), which does not occur only by thermal annealing. The chain conformation in these emptied crystals of sPS (γ, δ, and ε) is the same as that in cocrystals, which is different from that in crystals prepared by annealing in air (α and β). That is, sPS molecules can keep the history of the cocrystalline phase to a large extent despite the solvent removal. Tarallo et al. showed a detailed description of a channel type ε clathrate cocrystal of sPS.[16] They used *p*-nitroaniline as a guest, which is a highly polar molecule that makes its cocrystals possibly suitable for nonlinear optical and piezoelectric materials. Marubayashi et al. proposed that the formation of PLLA α''-crystals (quasi-stable phase) occurs as a result of CO_2 desorption from the PLLA−CO_2 complex in the cases of relatively low draw ratios.[6]

The guest exchange procedure helps host molecules form the complex with bulky guest molecules that cannot be encapsulated in the host by a single step. Uda et al. prepared the sPS clathrate containing organic dye (azulene) by the guest exchange procedure, and controlled the orientation of organic dye encapsulated in the sPS crystal.[17] Rizzo et al. presented chiral optical films based on sPS exhibiting stable circular dichroism (CD) phenomena also in the visible region, which can be easily obtained by inducing cocrystallization of sPS with suitable nonracemic guests and then exchanging the nonracemic guest with an achiral (or racemic) guest chromophore.[18] Yoshioka et al. proposed the solvent exchange mechanism in the sPS−solvent complex system.[19]

As mentioned above, we previously reported the complexation of PLLA with CO_2 and the specific organic solvents (ε-solvents), and their transition behavior with guest desorption.[6,9] At that time, PLLA *amorphous* films were exposed to the guest atmosphere (complexation from the *amorphous* state). In this study, we conducted an exhaustive research on *the crystal-to-crystal transitions of PLLA cocrystallized with low-molecular-weight compounds* using WAXD and Fourier transform infrared (FTIR) spectroscopy. First, the solvent exchange and the resultant transition behavior of solvent complexes are shown. We also demonstrate our trial to prepare the solvent complex consisting of PLLA and bulkier solvents compared with the ε-solvents by the solvent exchange procedure. Second, we show the crystal transition behavior between CO_2 and solvent complexes. Finally, the guest-induced transitions from non-complex crystals (α-, α'-, and α''-forms) are described (complexation from the *crystalline* state). Since PLLA has a structural similarity to poly(amino acid)s and polyhydroxyalkanoates (especially to poly(L-alanine) and poly[(*R*)-3-hydroxybutyrate], respectively), the insights obtained in this study are of great importance for better understanding of the molecular recognition ability of biobased polymers, leading to industrial applications such as separation and extraction polymeric materials with biocompatibility and biodegradability as well as processability.

EXPERIMENTAL SECTION

Samples. The PLLA used in this study is Lacty No. 5408 with a weight-average molecular weight (M_w) of 107 000 and an optical purity of 98.6%, and was supplied by the Toyota Motor Corp. For X-ray diffraction measurements, amorphous films with a thickness of 450 μm were prepared by melt pressing of the pellets at 200 °C and 20 MPa for 5 min and subsequent quenching by ice−water. The obtained films were confirmed to be completely amorphous by WAXD and differential scanning calorimetry. Organic solvents were used as received from commercial suppliers without further purification. The names and abbreviations of organic solvents we used are listed in Table 1. For infrared spectroscopic measurements, amorphous films with a thickness of 30 μm were prepared by solution casting (1 wt % $CHCl_3$ solution) and subsequent melt quenching. The obtained films were confirmed to be completely amorphous by the lack of the crystalline band in each infrared spectrum.

Table 1. Names and Abbreviations of Organic Solvents Used in This Study

name	abbrev
cyclohexanone	CHO
cyclopentanone	CPO
2,3-dihydrofuran	23DHF
1,3-dioxolane	DOL
γ-butyrolactone	GBL
γ-valerolactone	GVL
2-methyl-1,3-dioxolane	2MDOL
2-methyltetrahydrofuran	2MTHF
N,*N*-dimethylacetamide	DMAc
N,*N*-dimethylformamide	DMF
tetrahydrofuran	THF

Guest Exchange Procedures for PLLA Complexes. In the case of solvent−solvent exchange, first, the amorphous films were exposed to the ε-solvents, which were labeled as the "first solvents". Second, the resultant PLLA ε-films containing the

dx.doi.org/10.1021/jp308999t | J. Phys. Chem. B 2013, 117, 385−397

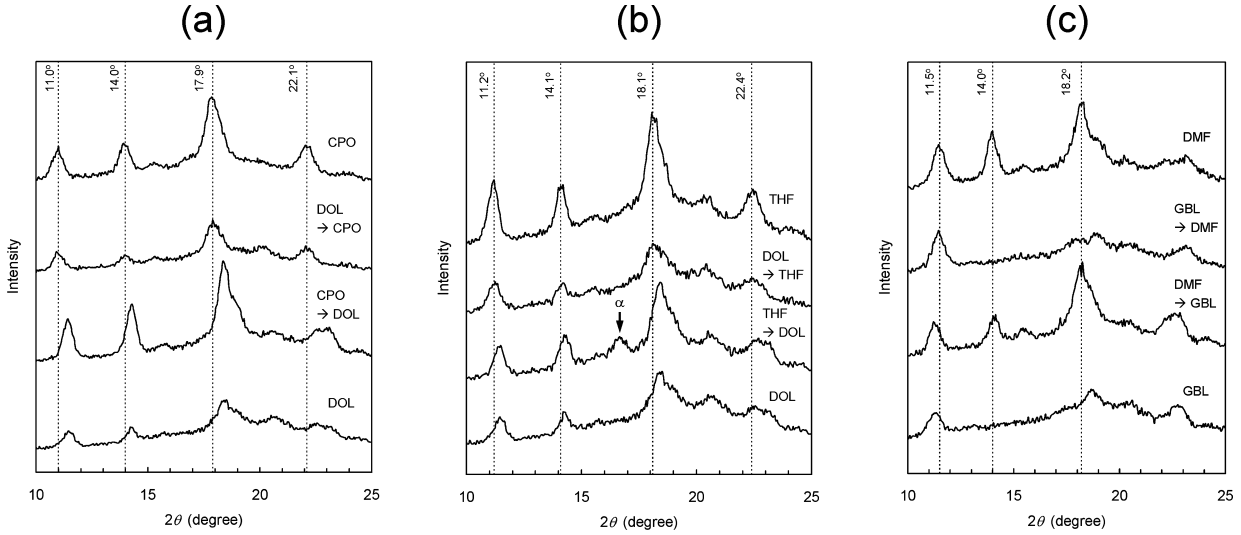

Figure 2. Change of WAXD curve by solvent exchange at −25 °C between (a) CPO and DOL, (b) THF and DOL, and (c) DMF and GBL.

first solvents (0.50−1.0 g/g_{PLLA}) were subjected to excess solvents that are different from the first solvents, which were referred to as the "second solvents". A ratio of the number of first solvents to that of second solvents was set to be smaller than 5%. Basically, the solvent exchange experiments were conducted at −25 and 25 °C. Because the PLLA we used dissolves in DOL at 25 °C,[9] the experiments in which DOL was set to the "second solvent" were performed only at −25 °C. Solvent exchange conditions are shown in the Supporting Information in detail.

For the guest exchange from solvent to CO_2, the PLLA films containing the ε-solvents were exposed to high-pressure CO_2 at 0 °C under 10 MPa for 2 h. As previously reported, when the amorphous film is subjected to high-pressure CO_2 in this condition, the formation of PLLA−CO_2 complex occurs.[6] The films just after the high-pressure CO_2 treatment were named the "as-taken films" irrespective of the initial state (i.e., amorphous or crystalline). The "low-temperature-stored films" were prepared by storing the as-taken films in air at 5 °C for 3−5 days. The "degassed films" were made by drying the low-temperature-stored films in a vacuum at room temperature for 1 week.

For the guest exchange from CO_2 to solvent, the low-temperature-stored films were exposed to the ε-solvent atmosphere at −25 and 25 °C.

Guest Exposure for Noncomplex Crystals. To examine the crystal transitions from noncomplex crystals to solvent complexes, the PLLA films having α-, α'-, and α''-crystals were used as the films having noncomplex crystals. The PLLA films having α-crystals were prepared by annealing in air at 140 °C for 5 h, while those having α'-crystals were prepared by annealing in air at 80 °C for 5 h. The α''-films (degassed films) were prepared by crystallization under 10 MPa CO_2 at 0 °C for 2 h, and subsequent CO_2 removal (storing at 5 °C for 3−5 days and vacuum drying at room temperature for 1 week), as mentioned above. PLLA α-, α'-, and α''-films were exposed to the ε-solvent atmosphere for 1−90 days depending on the volatility of each solvent. Solvent exposure temperatures were as follows: −25 and 25 °C for α''-film; −25 °C for α- and α'-films. To clarify the CO_2-induced transition behavior of noncomplex crystals, PLLA α-, α'-, and α''-films were exposed to high-pressure CO_2 at 0 °C under 10 MPa for 2 h.

Wide-Angle X-ray Diffraction (WAXD). One-dimensional WAXD measurements were conducted using a RINT-2100 (Rigaku Corp.) in a symmetrical transmission mode, equipped with a graphite monochromator ($2\theta_M$ = 26.58° for Cu Kα) at the scattered X-ray position. In an operating condition at 40 kV and 40 mA using Cu Kα (λ = 0.154 18 nm) as an X-ray source, X-ray radiation time was about 90 min for a single film (2θ = 3−50°, $\Delta(2\theta)$ = 0.05°). All measurements were carried out at room temperature under atmospheric pressure. Silicon powder was used as a standard sample. To minimize solvent evaporation, the PLLA films containing solvents were sealed by polyimide tapes during X-ray radiation.[9]

The weight ratio of the α-form in the crystalline region, X_α, was calculated from the following equation:

$$X_\alpha = \frac{A_\alpha}{A_\alpha + A_\varepsilon} \cdot 100 \quad (1)$$

where A_α is sum of areas of the α-derived peaks and A_ε is sum of areas of the ε-derived peaks. The peak separation was performed by using the handmade GUI software developed by Marubayashi (HerMesJ-1D[9]). The details are shown in the Supporting Information.

Fourier Transform Infrared (FTIR) Spectroscopy. FTIR spectra were measured using an FT/IR-620 (JASCO Corp.) with a resolution of 4 cm^{-1} and a cumulative number of 64 in air at room temperature for the solvent exchange. For the guest exchange from the ε-solvent to CO_2, FTIR measurements were performed with a resolution of 1 cm^{-1} and a cumulative number of 4 in air at room temperature. All FTIR measurements were conducted just after the guest exchange treatment.

RESULTS AND DISCUSSION

Crystal Transitions with Solvent Exchange. Figure 2 shows the changes in WAXD curves at 2θ of 10−25° before and after the solvent exchange experiments at −25 °C. Figure 3 shows the changes in IR spectra at 400−1000 cm^{-1} before and after the solvent exchange at −25 °C. Here, a labeling word of "solvent A" means the PLLA−"solvent A" complex film prepared by exposing the amorphous film to the "solvent A" atmosphere. In addition, "solvent A → solvent B" represents the PLLA−solvent complex film made by the solvent exchange

dx.doi.org/10.1021/jp308999t | J. Phys. Chem. B 2013, 117, 385−397

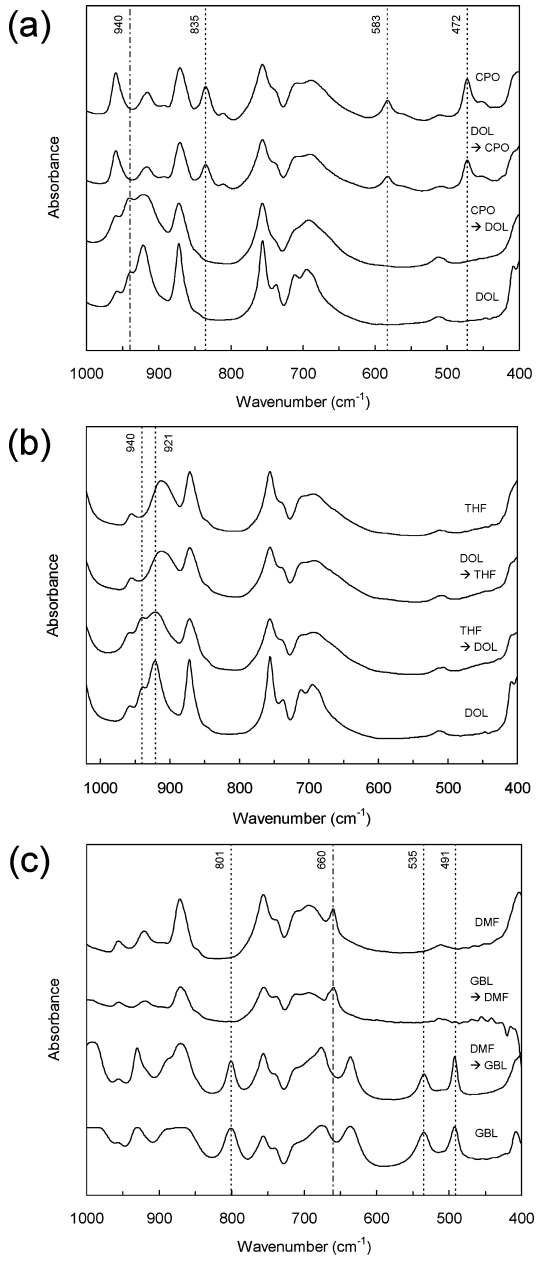

Figure 3. Change of FTIR spectrum by solvent exchange at −25 °C between (a) CPO and DOL, (b) THF and DOL, and (c) DMF and GBL.

in which solvent A is the first solvent and solvent B is the second solvent. Basically, for the solvent exchange between two ε-solvents selected from THF, DOL, CPO, and DMF, completion of the transition and the solvent exchange between two solvent complexes were confirmed by both WAXD (peak shift of each reflection derived from the first solvent) and FTIR (disappearance of IR bands derived from the first solvent and appearance of those derived from the second solvent) measurements. For example, the ε_{DOL}-derived diffraction peaks shifted to those of ε_{CPO} (e.g., $2\theta_{Cu\ K\alpha}$ = 11.0, 14.0, and 17.9°) by the solvent exchange (Figure 2a, DOL → CPO), and vice versa (Figure 2a, CPO → DOL). The diffraction peaks at $2\theta_{Cu\ K\alpha} \approx$ 11, 14, and 18° correspond to (200), (020), and (220)/(310) reflections of PLLA−solvent complexes, respectively ($d \approx$ 0.8, 0.6, and 0.5 nm, respectively).[9] In FTIR spectrum, the ε_{CPO}-derived IR bands (472, 583, and 835 cm^{-1}) disappeared and the ε_{DOL}-derived IR band (940 cm^{-1}) appeared by the solvent exposure to DOL (Figure 3a, CPO → DOL). On the other hand, the ε_{CPO}-derived bands were observable without the ε_{DOL}-derived band by exposing the PLLA−DOL complex film to CPO, as shown in Figure 3a (DOL → CPO). When THF was set as the first solvent, the transition to PLLA complex with the second solvent was often accompanied by the formation of a small number of α-crystals ($2\theta_{Cu\ K\alpha}$ = 16.7°; (110)/(200) reflection with d = 0.531 nm), as shown in Figure 2b (THF → DOL with X_α = 5.6%) and the Supporting Information (THF → CPO with X_α = 10.0%; THF → DMF with X_α = 4.7%). This result implies that desorption of THF from the film was superior to absorption of the second solvent. The lowest boiling point (T_b) of THF among the ε-solvents would support this suggestion. Here, the solvent exchange mechanism for PLLA−solvent complexes is discussed on the basis of that for sPS clathrates proposed by Yoshioka et al.[19] In the case of complexation of PLLA with DMF, PLLA chains form channel-shaped cavities, in which DMF molecules are encapsulated.[9] For simplicity, we assume that absorption of the second solvents preferentially occurs at one side of a PLLA lamella crystal, and desorption of the first solvents preferentially arises at the opposite side of the crystal. When the second solvents approach the PLLA lamella surface, the first solvents near the lamella surface would be driven from the current position. Since each channel surrounded by PLLA chains is not large enough for several solvents to pass, these first solvents should be driven from the near-surface region to the inner region of lamella crystal. As a result, the gradual desorption of the first solvents should arise at the opposite side of the lamella. As shown in Table 2, the unit cell volume of PLLA−solvent complex (V_{cpx}) increases with increasing molecular volume of the guest (V_{gst}). Therefore, the chain rearrangement of the host polymer (PLLA) needs to occur to encapsulate the second solvents in the cavity surrounded by hosts. For instance, in the case of the ε_{DOL}-to-ε_{CPO} transition, V_{cpx} increases by ca. 10%. The molecular models of ε-solvents are shown in Figure 4. If the absorption rate of the second solvents is comparable with the desorption rate of the first solvents, the solvent exchange in each channel will proceed without the formation of α-crystals. If desorption of the first solvents is superior to absorption of the second solvents, channel cavities without guests should be generated, resulting in the α-crystal formation due to the instability of the emptied structure.[9] This case corresponds to the solvent exchange starting from THF (Figure 2b and the Supporting Information).

Table 2. Molecular Volumes of ε-Solvents and Unit Cell Volumes of PLLA ε-Crystals

guest name	V_{gst}[a] (nm^3)	V_{cpx}[b] (nm^3)
CPO	0.0914	5.91
GBL	0.0800	5.60
THF	0.0760	5.58
DMF	0.0783	5.44
DOL	0.0696	5.42

[a]The molecular volumes of ε-solvents were obtained by the Connolly method[20] using Winmostar.[21] The molecular structure of each ε-solvent was obtained from gas-phase electron diffraction (CPO[22] and DMF[23]), ab initio calculation (DOL[24]), and X-ray diffraction (GBL[25] and THF[26]). [b]The unit cell volumes of PLLA−solvent complexes that were calculated from $V_{cpx} = abc$ (orthorhombic system).

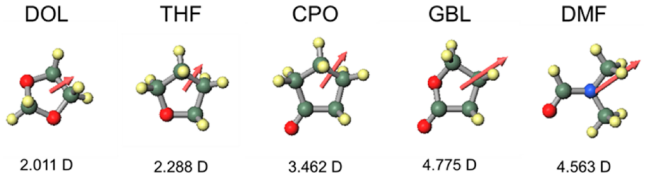

Figure 4. Molecular models of ε-solvents and their dipole moments (red arrows) that were drawn by Winmostar.[21] Calculated values of dipole moments for ε-solvents are also shown in Table 3.

In the case of solvent exchange containing GBL, the (200) peak position ($2\theta_{\mathrm{Cu\ K}\alpha} \approx 11°$, $d \approx 0.8$ nm) completely shifted to that of the second solvent, as shown in Figure 2c (GBL ↔ DMF) and the Supporting Information (GBL ↔ CPO; GBL ↔ DOL; GBL ↔ THF). For the (220)/(310) reflection ($2\theta_{\mathrm{Cu\ K}\alpha} \approx 18°$, $d \approx 0.5$ nm), however, such a complete peak shift was not observed even after the solvent exchange treatment for 1 month. In addition, when GBL was used as the second solvent, the (020) peak around 14° ($d \approx 0.6$ nm) was observable, while it is not seen in the unoriented GBL complex prepared directly from the unoriented amorphous state.[9] This result indicates that the periodicity parallel to the *b*-axis emerged in the GBL complex by the solvent exchange. It is considered that the emerged periodicity is responsible for disagreement in the (220)/(310) peak position between the $\varepsilon_{\mathrm{GBL}}$-films prepared from the amorphous and other ε-films. It seems likely that the periodicity parallel to the *b*-axis made by the first solvents still remains after the transition to the GBL complex. As previously reported, the (020) diffraction peak was also observed for the oriented GBL complex film.[9] The chain orientation given by drawing may induce the ordering in the *b*-axis direction. On the other hand, when GBL was set to the first solvent, the (020) peak was unobservable after the solvent exchange treatment. This result indicates that the disorder in the *b*-axis direction was not released by the second solvents (≠GBL). No periodicity parallel to the *b*-axis would account for disagreement in the (220)/(310) peak position after the solvent exchange. Why does the periodicity parallel to the *b*-axis change in the solvent exchange relating to GBL? In answer to this question, we suggest the occurrence of *orientational disorder* of GBL molecules encapsulated in PLLA crystals, which should induce the disordering in conformations of surrounding PLLA chains. The GBL-induced disordering of the host polymer should take place during the cooperative structural formation of hosts and guests (i.e., complexation) rather than after the complexation. As a result, the quasi-stable phase (ε') should be formed, in which no distinct periodicity in the *b*-axis direction is seen. Such disorder in the GBL direction might be due to the asymmetric molecular structure of GBL compared with other five-ring ε-solvents (CPO, DOL, and THF). In the cases of other five-ring ε-solvents (CPO, DOL, and THF), if the ring-puckering is neglected, we can find a 2-fold axis existing on the ring plane of each solvent, which is parallel to the dipole moment shown in Figure 4. On the contrary, there is no 2-fold axis on the ring plane of GBL, so some kinds of rotations in the internal coordinates of GBL give quite different positions of constituent atoms of GBL, although not so much for other five-ring ε-solvents. It should be possible to arrange GBL molecules without the periodicity parallel to the *b*-axis by some kinds of internal rotations, keeping the periodicity parallel to the *a*-axis. In addition, the highest T_b of GBL (≈200 °C) among the ε-solvents, in other words, the lowest molecular mobility of GBL, should also be responsible for the above-mentioned *orientational disorder*. For the solvent exchange starting from GBL, the solvent-complexed PLLA chains should be trapped in the quasi-stable phase due to the *orientational disorder* of GBL molecules. It seems likely that neither the conformational ordering of PLLA chains nor the *orientational ordering* of the second solvents ($\varepsilon' \rightarrow \varepsilon$) occurs despite the solvent exchange (disappearance of (020) reflection), indicating that the activation energy needed for the transition from ε' (quasi-stable) to ε (stable) is relatively high. On the other hand, when GBL was set to the second solvent, GBL molecules would drive the first solvents out from the channel-shaped cavities of PLLA, as discussed above. By the complexation with the first solvents (≠GBL), there would be the periodicity parallel to the *b*-axis (ε-form), where the *orientational disorder* in the first solvents should be small enough to be neglected, if any. Since the system has already been the stable state (ε) before the solvent exchange treatment, GBL penetration into a film would yield the PLLA–GBL complex having the periodicity in the *b*-axis direction ($\varepsilon_{\mathrm{GBL}}$, appearance of (020) reflection), without the conformational disordering of PLLA.

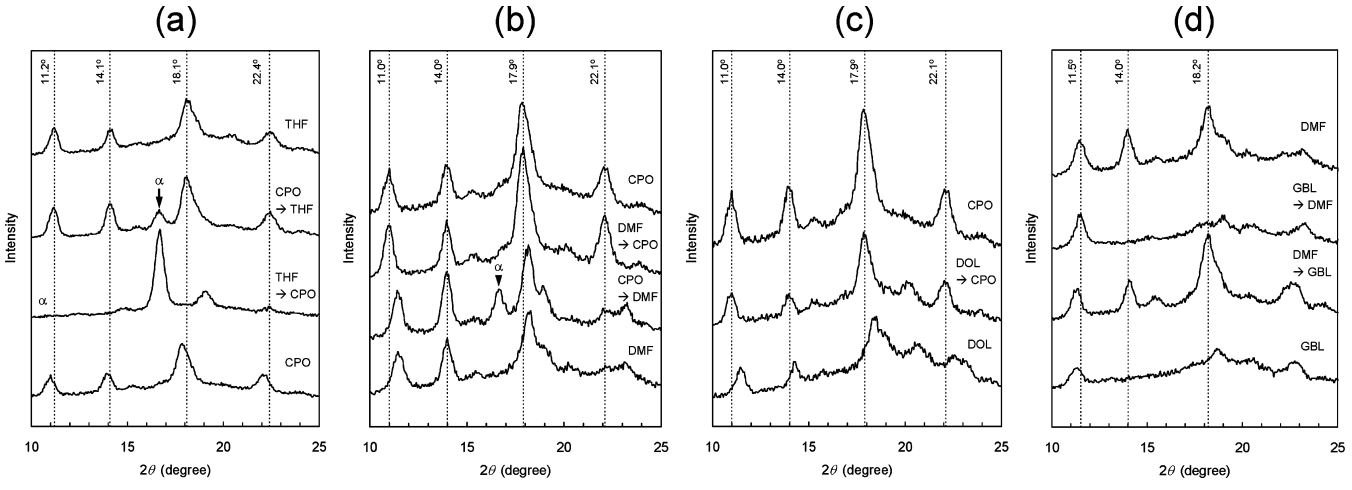

Figure 5. Change of WAXD curve by solvent exchange at 25 °C between (a) THF and CPO, (b) CPO and DMF, (c) CPO and DOL, and (d) DMF and GBL.

dx.doi.org/10.1021/jp308999t | J. Phys. Chem. B 2013, 117, 385–397

In the solvent exchange containing GBL, IR bands derived from the first solvent almost perfectly disappeared by the solvent exchange (e.g., Figure 3c, GBL ↔ DMF). In the cases of solvent exchange from GBL to THF (Supporting Information, GBL → THF) and from GBL to CPO (Supporting Information, GBL → CPO), the GBL-derived band (491 cm^{-1}) was still observed with considerably small absorbance even after the solvent exchange treatment for 1 month.

Figure 5 shows the changes in WAXD curves at 2θ of 10–25° before and after the solvent exchange experiments at 25 °C. On the whole, with increasing the solvent exchange temperature from −25 to 25 °C, there was an increase in the ratio of the α-form in the crystalline region in the resultant film. In particular, the ε_{THF}-form showed the complete transition to the α-form (i.e., X_α = 100%) by the solvent exchange treatment at 25 °C, as shown in Figure 5a (THF → CPO) and the Supporting Information (THF → DMF; THF → GBL). When the CPO complex was the first solvent, the transition to the complex of the second solvent was accompanied by the formation of a small number of α-crystals, as seen in Figure 5a (CPO → THF, X_α = 7.5%), Figure 5b (CPO → DMF, X_α = 7.0%), and the Supporting Information (CPO → GBL, X_α = 8.5%). On the contrary, the other three solvent complexes (DMF, DOL, and GBL) still showed the complete transition to the complex of the second solvent without the formation of α-crystals (i.e., X_α = 0%), as shown in Figure 5b (DMF → CPO), Figure 5c (DOL → CPO), Figure 5d (GBL → DMF; DMF → GBL), and the Supporting Information (DMF → THF; DOL → DMF; DOL → GBL; DOL → THF; GBL → CPO; GBL → THF). When GBL was set to the first solvent, the periodicity parallel to the *b*-axis changed by the solvent exchange at 25 °C (e.g., Figure 5d), as is the case with solvent exchange at −25 °C. As previously reported, exposure of the amorphous PLLA to the ε-solvents at 25 °C yields only the α-form (non-complex).[9] On the contrary, it was found that the PLLA–solvent complexes (CPO, DMF, GBL, and THF) themselves, once formed below room temperature, are stable in the ε-solvent atmosphere at room temperature (25 °C). As mentioned above, it was observed that X_α (the ratio of the α-form in the crystalline region) after the solvent exchange increases with increasing the surrounding temperature from −25 to 25 °C. This phenomenon should be explained by an enhanced unbalance between desorption of the first solvents and absorption of the second ones at 25 °C.

Substitution of a CH_3 group for a hydrogen atom in each ε-solvent hinders the formation of solvent complexes.[9] We tried to make the solvent complexes of PLLA with the CH_3-substituted ε-solvents by the solvent exchange method, in which the first solvents were the ε-solvents and the second ones were the CH_3-substituted ε-solvents. Unfortunately, all solvent complexes showed the transition to the α-form by this method, as shown in Figure 6 (−25 °C) and the Supporting Information (25 °C). Even by the introduction of one unsaturated carbon bond (2,3-dihydrofuran and 2,5-dihydrofuran), the formation of solvent complexes does not occur.[9] The solvent exchange from THF to 2,3-dihydrofuran resulted in the transition from the THF complex to the α-form (Figure 6). Thus, we failed to prepare the solvent complex of PLLA with 2,3-dihydrofuran by the solvent exchange technique. Although we failed to make PLLA cocrystallized with non-ε-solvents by the solvent exchange method, it was confirmed that PLLA possesses high selectivity for low-molecular-weight compounds to form ε-crystals.

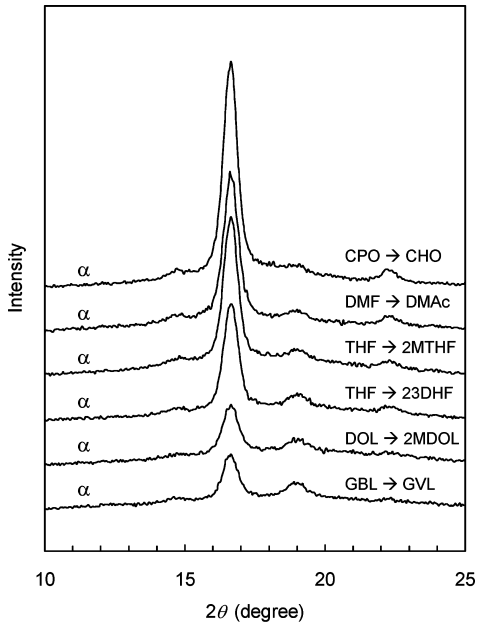

Figure 6. Change of WAXD curve by solvent exchange between ε-solvent and its derivative at −25 °C.

The crystal-to-crystal transitions between any two forms selected from the ε-forms (PLLA–solvent complexes) are summarized in Figure 7. Here, we discuss these transition behaviors on the basis of the Hansen solubility parameter (HSP)[27–29] of the ε-solvents. The total solubility parameter (δ_t), which corresponds to the Hildebrand solubility parameter, is given by the following equation:[27]

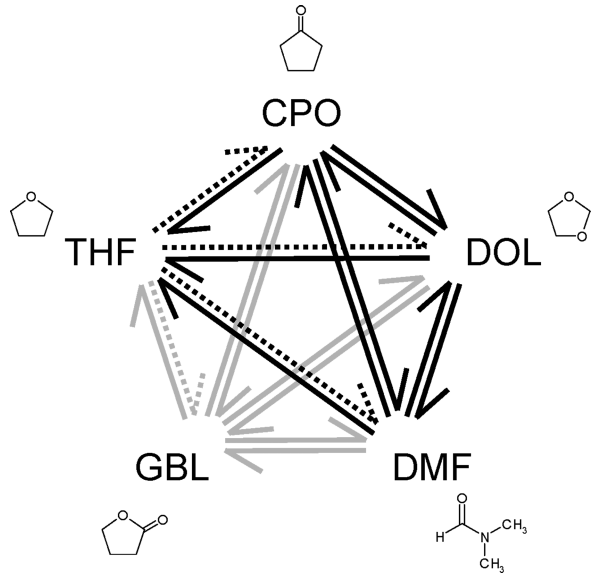

Figure 7. Schematic illustration showing the transition behavior among PLLA–solvent complexes at −25 °C. Solid line shows that transition between solvent complexes was completed without formation of α-crystals. Broken line represents that transition between solvent complexes was accompanied by formation of α-crystals. Solvent exchange containing GBL is distinguished by gray line, because of changes in the periodicity parallel to the *b*-axis by solvent exchange.

dx.doi.org/10.1021/jp308999t | J. Phys. Chem. B 2013, 117, 385–397

Table 3. Hansen Solubility Parameters, Relative Energy Differences, Dipole Moments, and Boiling Points of ε-Solvents

name	δ_d[a] (MPa$^{1/2}$)	δ_p[a] (MPa$^{1/2}$)	δ_h[a] (MPa$^{1/2}$)	δ_t[a] (MPa$^{1/2}$)	RED	μ[b] (D)	T_b (°C)
THF	16.8	5.7	8.0	19.5	0.54	2.288	65
DOL	18.1	6.6	9.3	21.4	0.44	2.011	75
CPO	17.9	11.9	5.2	22.1	0.25	3.462	130
DMF	17.4	13.7	11.3	24.9	0.67	4.563	153
GBL	19.0	16.6	7.4	26.3	0.68	4.775	204
PLLA	18.5	9.7	6.0	21.7	–	–	–

[a]Solubility parameters of ε-solvents and PLLA obtained from refs 28 and 29, respectively. [b]Dipole moments obtained by the single point calculations of MOPAC 2012 using PM6 Hamiltonian.[30] Molecular models of ε-solvents were same as those used in Table 2.

$$\delta_t = \sqrt{\delta_d^2 + \delta_p^2 + \delta_h^2} \quad (2)$$

where δ_d is the solubility parameter due to dispersion forces, δ_p is the solubility parameter due to dipole forces, and δ_h is the solubility parameter due to hydrogen bonding. Table 3 shows HSPs of the ε-solvents[28] and PLLA.[29] Comparable δ_d values (16.8−19.0 MPa$^{1/2}$) were obtained for the ε-solvents, whereas there were distinct differences in δ_p (5.7−16.6 MPa$^{1/2}$) and δ_h (5.2−11.3 MPa$^{1/2}$) depending on the combination of any two ε-solvents. The solvent polarity was estimated not only by δ_p but also by the dipole moments (μ), as also shown in Table 3. The molecular models of ε-solvents with the calculated dipole moments were previously shown in Figure 4. A similar trend was observed in δ_p and μ. The distance in three-dimensional solubility space between polymer and solvent (R_a) can be calculated from eq 3, whose maximum tolerable value for solution to take place corresponds to the radius of the interaction sphere (R_0).[27−29]

$$R_a = \sqrt{4(\delta_{dp} - \delta_{ds})^2 + (\delta_{pp} - \delta_{ps})^2 + (\delta_{hp} - \delta_{hs})^2} \quad (3)$$

where the second characters in subscripts "p" and "s" represent polymer and solvent, respectively. The value of R_a/R_0 is termed the relative energy difference (RED),[27,28] where R_0 of PLLA is 10.50 MPa$^{1/2}$.[29] The values of RED lower than 1 indicate good solvents for the polymer, while those higher than 1 indicate poor solvents. As seen in Table 3, all ε-solvents possess RED values smaller than 1 (i.e., good solvents for PLLA). Thus, in addition to the size, shape, and functional groups of solvents,[9] RED smaller than 1 was found to be necessary in the ε-crystal formation. In this study, only DOL dissolved PLLA at room temperature, which should be attributed to the relatively high molecular weight of PLLA used ($M_w \approx 1 \times 10^5$ and $DP_w \approx 1500$). Thus, it was experimentally confirmed that DOL possesses the highest affinity for PLLA among the ε-solvents. In terms of subgeneration of α-crystals in the solvent exchange, a distinct difference was observed between THF and DOL despite comparable T_b (molecular mobility). This result implies that the PLLA−DOL interaction, which would be stronger than the PLLA−THF interaction, hinders the preferential desorption of DOL molecules from PLLA cocrystals during the solvent exchange, leading to no subgeneration of α-crystals. Accordingly, it should be reasonable to consider that the affinity of solvent for PLLA as well as the molecular mobility of solvent (T_b) has a great effect on phase transitions among PLLA−solvent complexes.

As mentioned above, we suggested that the asymmetric molecular structure of GBL has an effect on the specific transition behavior in the solvent exchange. As seen in Figure 4, DMF also has the same kind of asymmetry. When the HSP values of DMF and GBL are compared, δ_p of the former (13.7 MPa$^{1/2}$) is smaller than that of the latter (16.6 MPa$^{1/2}$), and δ_h of the former (11.3 MPa$^{1/2}$) is higher than that of the latter (7.4 MPa$^{1/2}$). Thus, DMF has relatively high δ_p and δ_h (both HSP values >10 MPa$^{1/2}$), which is special among good solvents of PLLA.[29] The directionality of hydrogen bonding should be responsible for the *orientational ordering* of DMF molecules in PLLA cocrystals, resulting in the periodicity parallel to the *b*-axis direction, unlike the PLLA−GBL complex. Furthermore, the higher molecular mobility of DMF (T_b = 153 °C) compared with GBL (T_b = 204 °C) would also hinder the *orientational disordering*.

Crystal Transitions between Solvent and CO_2 Complexes. First, the transition from solvent to CO_2 complexes is discussed. Figure 8 shows the change of the WAXD curve by the high-pressure CO_2 treatment for the ε-films. The complete transition from solvent to CO_2 complexes was able to be seen for all solvent complexes, although there was a small discrepancy in the peak position between the as-taken film prepared from the amorphous film and that prepared from the solvent complex. In the case of high-pressure CO_2 treatment for the GBL complex, the (200) reflection of CO_2 complex around 19° was not clearly observed. Interestingly, for the CO_2 complex prepared from the DMF complex, the diffraction intensity significantly increased compared with the CO_2 complex prepared from the amorphous state. If absorption of

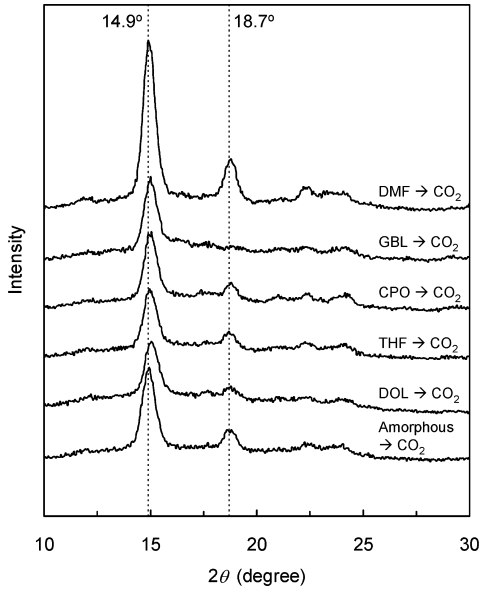

Figure 8. Change of WAXD curve by exposing ε-films to high-pressure CO_2. WAXD measurements were conducted just after high-pressure CO_2 treatments.

dx.doi.org/10.1021/jp308999t | J. Phys. Chem. B 2013, 117, 385−397

CO_2 molecules into PLLA crystals occurs after desorption of solvents (ε-to-α), the CO_2 complex film without other crystal polymorphs will not be obtained. Exposure of the α-film to high-pressure CO_2 gave the mixture of CO_2 complex and other crystal forms, as shown later in detail. Hence, it should be reasonable to assume that the solvent desorption and CO_2 absorption occur simultaneously, which would be supported by the high diffusivity of pressurized CO_2. Since the molecular volume of CO_2 (0.0332 nm^3; the molecular structure from single-crystal X-ray diffraction[31]) is much smaller than those of ε-solvents (0.0696−0.0914 nm^3; Table 2), the rearrangement of PLLA chains and CO_2 molecules should occur to take a denser packing style and have stronger interactions, resulting in the formation of PLLA−CO_2 complex. Furthermore, the change in the FTIR spectrum by the high-pressure CO_2 treatment for the ε-films is shown in the Supporting Information. After the ε-films were exposed to pressurized CO_2, no solvent-derived bands were seen and the CO_2 ν_2 bending bands[6b,32] at 650−670 cm^{-1} appeared. Thus, completion of the transition from solvent to CO_2 complexes was confirmed by both WAXD and FTIR.

Next, the transition from CO_2 complex to solvent complex is focused. When the low-temperature-stored film was exposed to THF at −25 °C, the diffraction peak at 16.6° as well as those derived from the THF complex was observed (Figure 9a). The ratio of the former (16.6°) in the crystalline region, which was calculated in the same manner as X_α, is 24.8%. Even after exposure to CPO, DMF, or GBL at −25 °C for 3 months, the diffraction peaks derived from the solvent complex were unobservable, and a fairly large proportion of CO_2 complex crystals remained, as shown in Figure 9b (exposure to CPO). The diffraction peak at 16.6°, which is not derived from the solvent complex, slightly increased in intensity with increasing exposure time. This would be due to poor absorption of these solvents with relatively high T_b (>100 °C) to the CO_2 complex film at a relatively low temperature (−25 °C), which was confirmed by the weighing of each film. On the other hand, when subjected to the ε-solvents at 25 °C for 2 weeks, the CO_2 complex showed a complete transition to the α-form, as shown in Figure 10. For the unoriented PLLA film, the CO_2 complex does not exhibit the transition to α-form without annealing in air around T_g of PLLA (the transition stops at the emptied form, α'').[6b] Therefore, at 25 °C, the ε-solvents might assist the transition from the CO_2 complex to the α-form just as a plasticizing agent. This result would be explained by an increase in the molecular mobility of both PLLA chains and solvent molecules with increasing the solvent exposure temperature. Such a complete crystal transition to the α-form should hinder the transition to the solvent complex, as demonstrated later.

Figure 11a shows the time-dependent change of the WAXD curve by exposure of the low-temperature-stored film to DOL at −25 °C. Figure 11b exhibits the changes in peak areas for the representative reflections of the CO_2 complex, α_1-form (defined below), and ε_{DOL}-form. It was difficult to obtain the ratio of each crystalline phase quantitatively because of overlapping of several peaks and their broadness. As an alternative, a qualitative change of each crystalline phase was evaluated by using areas of the selected peaks. With increasing exposure time, intensity of the (110) reflection of the CO_2 complex ($2\theta_{Cu\ K\alpha}$ = 15.2°, d = 0.583 nm) decreased. Simultaneously, the diffraction peak at 16.6° (d = 0.534 nm) appeared and increased in intensity (DOL exposure period of 1−6 h). After that, diffraction peaks derived from the DOL complex appeared

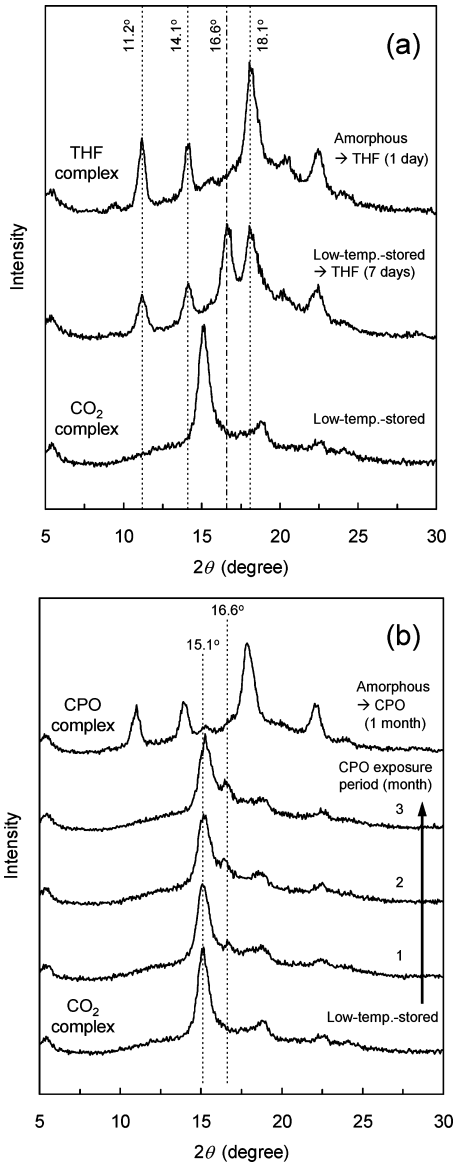

Figure 9. Change of WAXD curve by exposure of low-temperature-stored film (CO_2 complex) to (a) THF and (b) CPO atmospheres at −25 °C.

and increased in intensity (≥12 h). After it was subjected to the DOL atmosphere for 24 h, the (110) reflection of the CO_2 complex was no longer observed. Simultaneously, the intensity of the diffraction peak at 16.6° drastically decreased (18 → 24 h). Finally, only the ε_{DOL}-derived peaks were observed after DOL exposure for 168 h (complete transition to PLLA−DOL complex). Thus, it was found that the crystal transition from the CO_2 complex to the DOL one occurs via another crystal polymorph (2θ = 16.6°, d = 0.534 nm), which is referred to as the "α_1-form" for convenience. This "α_1-form" would be a structure quite similar to the α-form (2θ = 16.7°, d = 0.531 nm). The possibility that the "α_1-form" is the mixture of α- and α'-forms (2θ = 16.7 and 16.5°, respectively) would be denied, because the α-to-DOL complex transition was not seen, as mentioned later in detail. In the early stage of the transition from CO_2 to DOL complexes, it seems that the CO_2 complex changes to the "α_1-form" by CO_2 desorption from PLLA cocrystals, resulting in a decrease in the unit cell volume. After that, it is likely that penetration of DOL molecules into free

dx.doi.org/10.1021/jp308999t | J. Phys. Chem. B 2013, 117, 385−397

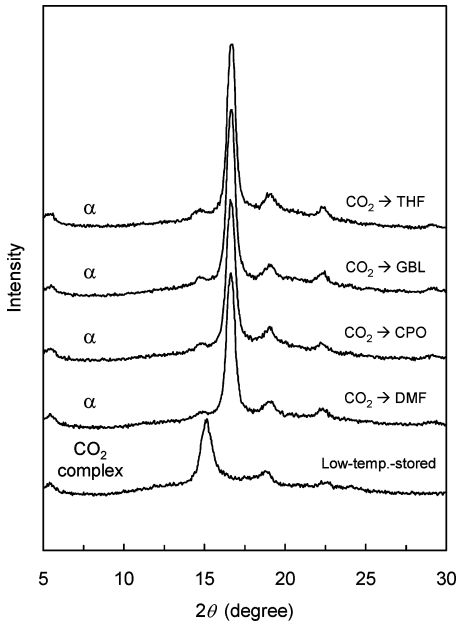

Figure 10. Change of WAXD curve by exposure of low-temperature-stored film to ε-solvents except DOL at 25 °C. Exposure to THF, CPO, and DMF atmospheres was performed for 1 week. GBL exposure was conducted for 2 weeks.

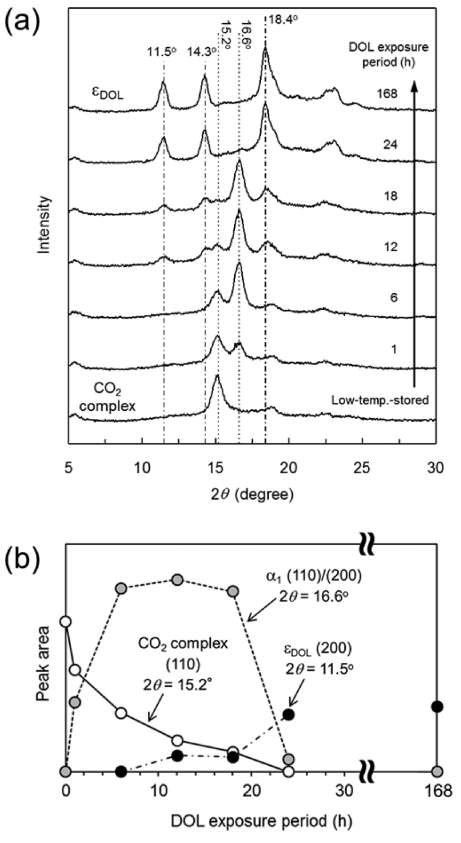

Figure 11. (a) Temporal change of WAXD curve by exposure of low-temperature-stored film to DOL atmosphere at −25 °C. (b) Changes in areas of selected peaks of CO_2 complex ((110), 2θ = 15.2°, d = 0.583 nm), α_1-form ((110)/(200), 2θ = 16.6°, d = 0.534 nm), and ε_{DOL}-form ((200), 2θ = 11.5°, d = 0.769 nm) as a function of DOL exposure period.

spaces (cavities) in PLLA crystals occurs, followed by the rearrangement of PLLA chains by the PLLA−DOL complexation. As mentioned later, a small improvement in the chain packing ($\alpha > \alpha' > \alpha''$) had a large effect on the noncomplex-to-DOL complex transition, i.e., DOL penetration into PLLA crystals. Based on this result, the slightly poor chain packing of the "α_1-form" compared with the α-form should help DOL molecules penetrate into cavities in PLLA crystals. When the low-temperature-stored film (CO_2 complex) was subjected to the CPO, DMF, or GBL atmosphere at −25 °C, the small diffraction peak derived from "α_1-crystals" was also able to be seen, as mentioned above (Figure 9b). However, it is considered that the transition from the "α_1-form" to solvent complex (CPO, DMF, or GBL) does not occur, because the transition from the α'-form (2θ = 16.5°, d = 0.537 nm) to solvent complex was not observed for these solvents even after exposure for 1 month (shown in the section Solvent-Induced Transitions from Noncomplex Crystals). Here, the ratio of "α_1-crystals" in the crystalline region was ca. 25% for the THF case (Figure 9a), which is much smaller than that for the case of CO_2 complex → DOL complex at 12−18 h (Figure 11). This result implies that the absorption−desorption balance of the former is better than that of the latter, although completion of the transition to solvent complex without subgeneration of other crystal polymorphs was obtained only in the latter case.

Solvent-Induced Transitions from Noncomplex Crystals. When the films having the disordered α-crystals (α' and α'') were exposed to the ε-solvents, in some cases, the crystal transition to the ε-form occurred. In the case of solvent exposure starting from the α'-crystal, only DOL molecules penetrated into the α'-film and assisted the α'-to-ε_{DOL} transition, as shown in Figure 12a. On the contrary, the α-to-ε transition was not observed by exposure of the α-films to the ε-solvent atmosphere for a long time (Figure 12b), although the difference between the α- and α'-forms is relatively small in terms of the lattice constants. The chain conformation of the α'-form is more remarkably disordered than that of the α-form.[5a] The α'-domains constructed by the alternate arrangement of upward and downward chains are gathered together with the mismatch in the relative height between the neighboring domains.[5a] It would be reasonable to consider that DOL molecules become easy to penetrate into PLLA crystals by an increase in the structural disorder. In addition to such a difference in the crystal structure, the discrepancy in crystallinity between the α- and α'-films may have an effect on the difference in their transition behavior.

In the case of solvent exposure starting from the α''-crystal (degassed films) at −25 °C, the crystal-to-crystal transition behavior showed the solvent species dependence. First, by exposure to the DOL atmosphere at −25 °C, the α''-form showed the transition to the ε-form (Figure 13a). In the early stage of transition (1 h; not shown), the diffraction peak shifted from 16.2° (α'') to 16.6°. With increasing exposure time to DOL, the intensity of the peak at 2θ = 16.6° decreased and peaks derived from ε_{DOL} (e.g., 2θ = 11.5, 14.3, and 18.4°) increased in intensity. It should be noted that the position of the resulting peak (16.6°) was slightly lower compared with that of the α-form (16.7°). This result indicates that the formation of "α_1-crystals" occurred during the α''-to-DOL complex transition, as in the CO_2 complex-to-DOL complex transition at −25 °C (Figure 11). Second, when exposed to THF at −25 °C, the α''-film gave a mixture of α- and ε-forms, as shown in Figure 13b (X_α = 14.9%). The subsequent

dx.doi.org/10.1021/jp308999t | J. Phys. Chem. B 2013, 117, 385−397

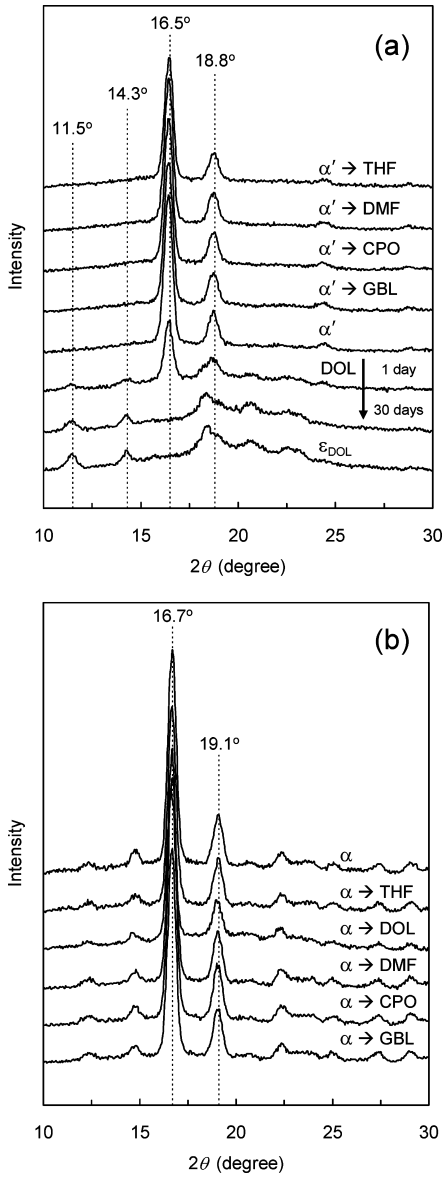

Figure 12. Change of WAXD curve by exposure of (a) α'- or (b) α-film to the ε-solvent atmosphere. Solvent exposure periods were set to 14 days for CPO and 30 days for other solvents. Exposure temperature was set to 5 °C for CPO and −25 °C for others.

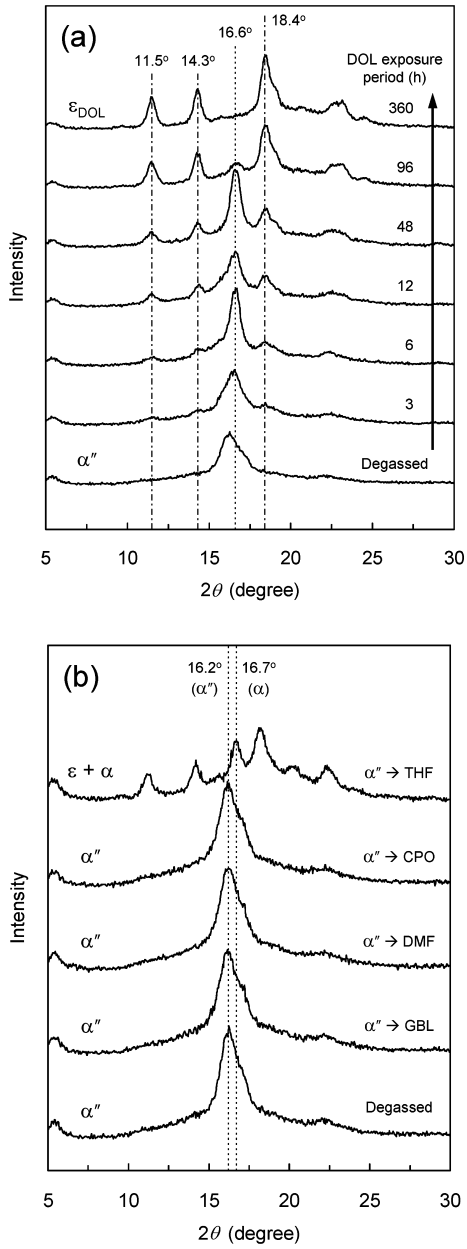

Figure 13. Change of WAXD curve by exposure of degassed film to (a) DOL or (b) other ε-solvents at −25 °C. (b) Solvent exposure period was 2 months.

transition from the resultant α-form to other crystal polymorphs was not observed. Finally, in the cases of CPO, DMF, and GBL at −25 °C, there were almost no changes in WAXD curves even after solvent exposure of the α''-film for 2 months (Figure 13b). Poor solvent penetration into the film (10−30 mg/g_{PLLA}) for these three solvents should be the cause of no changes in the crystal structure.

It appears that DOL is special among the ε-solvents in terms of structure transitions from the noncomplex crystals (i.e., the complete transition from the disordered α to ε_{DOL} with no subgeneration of α-crystals). As mentioned above, PLLA used in this study dissolves in DOL at room temperature, but not in other ε-solvents.[9] Such a high affinity of DOL for PLLA should be responsible for the specific phase transition behavior (i.e., penetration into the α'- and α''-films, and the assistance of the transition to ε_{DOL} without the α-crystal formation). Poor penetration of CPO, DMF, and GBL into the noncomplex crystal films would be due to lower affinity for PLLA and higher T_b (i.e., lower molecular mobility) compared with DOL. Unlike the solvent exchange experiments in which the first solvents were in both the crystalline (solvent complexes) and amorphous (swollen state) regions of PLLA, it is considered that the high-T_b ε-solvents stop at the surface region of a film, because each PLLA amorphous domain is surrounded by the lamellae of noncomplex crystals into which these solvents are difficult to penetrate. In the case of THF, penetration into a film was improved by relatively high molecular mobility (relatively low T_b), although the transition to ε_{THF} was accompanied by the generation of α-crystals due to lower affinity for PLLA compared with DOL.

When subjected to the ε-solvents at 25 °C, the α''-form showed the transition to the α-form, not via the ε-forms or other crystal modifications, as shown in the Supporting

dx.doi.org/10.1021/jp308999t | J. Phys. Chem. B 2013, 117, 385−397

Information. In other words, the ε-solvents induced only the α''-to-α transition at room temperature.

CO_2-Induced Transitions from Noncomplex Crystals. Figure 14 shows the change of the WAXD curve by the CO_2-induced transitions for various noncomplex films. Diffraction peak positions and intensities of the as-taken film prepared from the α''-film were in fairly good agreement with those of the as-taken film prepared from the amorphous film. Thus, it was found that there is reversibility between the CO_2 complex and the α''-form by the CO_2 absorption/desorption. In the case of CO_2 treatment for the α'-film, the diffraction peak intensity (especially for the (110) reflection at $2\theta \approx 15°$) decreased compared with the as-taken film prepared from the amorphous one. In addition, the diffraction angle of the (110) reflection was slightly higher than that for the as-taken film prepared from the amorphous one ($2\theta = 14.9°$, $d = 0.595$ nm). Furthermore, a small shoulder was observable around $2\theta = 16.4°$, which was not seen in the CO_2 complex film made from the amorphous one. In the WAXD curve of the as-taken film prepared from the α-film, the diffraction peak at $2\theta = 16.4°$ as well as the (110) and (200) reflections of the CO_2 complex was observed. This diffraction peak ($2\theta = 16.4°$, $d = 0.540$ nm) showed almost constant intensity irrespective of the CO_2 treatment time (2, 12, and 24 h). Thus, it was found that the transition from noncomplex to CO_2 complex becomes difficult to occur with increasing order of the crystal ($\alpha > \alpha' > \alpha''$). This result can be explained by the idea that CO_2 molecules become more difficult to penetrate into free spaces (cavities) in PLLA crystals by a denser chain packing. Because the α-form is the most stable and has the densest chain packing among these three polymorphs, the activation energy need for the transition from noncomplex to CO_2 complex should be largest. Although structural differences among these noncomplex crystals are considered to be not so large judging from the chain conformation, packing, and unit cell dimensions,[3,5,6] the CO_2-induced transition behavior from noncomplex crystals was much influenced by the selected noncomplex.

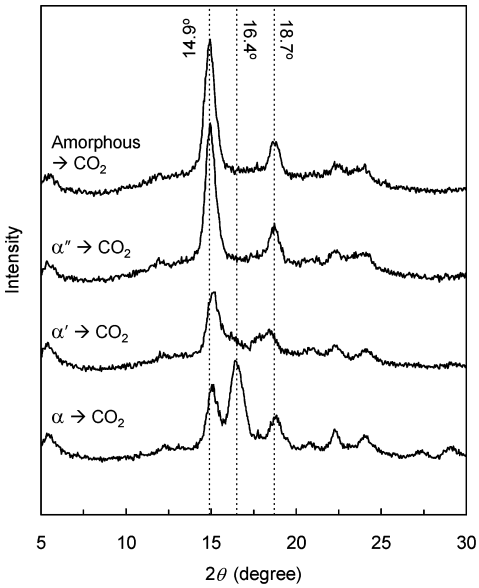

Figure 14. Change of WAXD curve by CO_2-induced crystal−crystal transition for various crystallized films. CO_2 treatment time was set to 2 h for all films.

Finally, the crystal-to-crystal transition behavior between two polymorphs selected from the PLLA−CO_2 complex, PLLA−solvent complexes, and noncomplex crystals (α, α', and α'') is shown in Figure 15.

CONCLUSIONS

In this article, various kinds of crystal-to-crystal transitions relating to PLLA cocrystallized with low-molecular-weight compounds (CO_2 and ε-solvents) were examined in a systematic way using WAXD and FTIR.

First, the solvent exchange and the resultant transition behavior of solvent complexes were investigated using WAXD and FTIR. Basically, by the solvent exchange treatments between two solvents selected from CPO, DMF, DOL, and THF, the solvent exchange and the crystal transition were found to be completed. In the case of solvent exchange containing GBL, it was found that the periodicity parallel to the b-direction of PLLA−solvent complex is much affected by whether GBL was set to the first solvent (quasi-stable phase, ε') or not (stable phase, ε). With increasing solvent exchange temperature, the ratio of the α-form in the crystalline region increased in the resultant film, especially in the solvent exchange in which THF was set to the first solvent. The mechanisms of solvent-exchange-induced phase transitions were discussed in terms of the absorption−desorption kinetics, molecular mobility, and solubility parameters of the ε-solvents. We failed to prepare the solvent complex consisting of PLLA and bulkier solvents compared with the ε-solvents by the solvent exchange procedure (ε-to-α transition), indicating the high selectivity of PLLA for low-molecular-weight compounds.

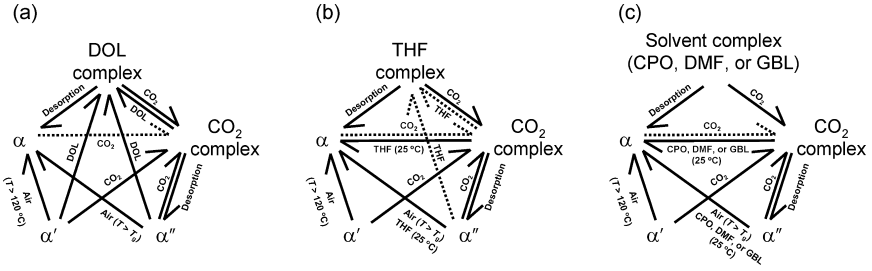

Figure 15. Schematic illustration showing the transition behavior between two polymorphs selected from the solvent complex, CO_2 complex, and noncomplex crystals (α, α', and α''). (a) DOL exposure was conducted only at −25 °C. (b) THF without labeling of temperature (e.g., CO_2 complex → THF complex) means THF exposure at −25 °C. (c) Results of exposure to CPO, DMF, and GBL at −25 °C were not shown, because of relatively low solubility of these three solvents in the PLLA film at −25 °C. Each broken line represents that completion of the transition was not obtained (mixture with other crystal structure).

dx.doi.org/10.1021/jp308999t | J. Phys. Chem. B 2013, 117, 385−397

Second, we examined the crystal transition behavior between CO_2 and solvent complexes. The transition from solvent to CO_2 complexes occurred for all solvent complexes. In contrast, it was found that the transition behavior from CO_2 to solvent complexes is much influenced by types of solvents and the surrounding temperature. Completion of the transition was observable only for the CO_2 → DOL case (−25 °C). It was indicated that the diffusivity and affinity of solvent to PLLA have a great effect on the transition behavior from CO_2 to solvent complexes.

Finally, the guest-induced transitions of noncomplex crystals (α-, α'-, and α''-forms) were investigated. As a result, it was found that species of noncomplex crystals (α, α', and α'') as well as kinds of guest molecules have a great effect on the guest-induced transition behavior of noncomplex crystals.

■ ASSOCIATED CONTENT

Supporting Information

Solvent exchange conditions (Table S1); an example of peak separation for WAXD curve of the ε-film with a small number of α-crystals (Figure S1); the change of WAXD curve by the solvent exchange at −25 °C (Figure S2); the change of FTIR spectrum by the solvent exchange at −25 °C (Figure S3); the change of WAXD curve by the solvent exchange at 25 °C (Figure S4); the change of WAXD curve by the solvent exchange between ε-solvent and its derivative at 25 °C (Figure S5); the change of IR spectrum by exposure of ε-films to high-pressure CO_2 (Figure S6); the change of WAXD curve by exposing the degassed film (α'') to the ε-solvents except DOL at 25 °C (Figure S7). This material is available free of charge via the Internet at http://pubs.acs.org.

■ AUTHOR INFORMATION

Corresponding Author

*Tel.: +81-3-5734-2432. Fax: +81-3-5734-2431. E-mail: asai.s.aa@m.titech.ac.jp.

Notes

The authors declare no competing financial interest.

‡Research Fellow of the Japan Society for the Promotion of Science.

■ ACKNOWLEDGMENTS

H.M. thanks Prof. K. Tashiro (Toyota Technological Institute), Prof. T. Ozeki (Tokyo Institute of Technology), Prof. P. D. Hong (National Taiwan University of Science and Technology), Prof. O. Tarallo (Università degli Studi di Napoli Federico II), Prof. M. Wada (The University of Tokyo), and Dr. H. Shii for giving him beneficial suggestions. We thank the Toyota Motor Corp., Japan, for supplying the PLLA pellets. Financial support from the Tokyo Institute of Technology Global COE program "Education and Research Center for Emergence of New Molecular Chemistry" is gratefully acknowledged. This work was partly supported by a Grant-in-Aid for JSPS Fellows (No. 22008912) from Japan Society for the Promotion of Science.

■ REFERENCES

(1) (a) Gandini, A. *Macromolecules* **2008**, *41*, 9491−9504. (b) Coates, G. W.; Hillmyer, M. A. *Macromolecules* **2009**, *42*, 7987−7989. (c) *Bio-Based Polymers: Recent Progress*; Im, S. S., Kim, Y. H., Yoon, J. S., Chin, I.-J., Eds.; Macromolecular Symposia; Wiley-VCH: Weinheim, Germany, 2005. (d) *Biodegradable Polymers and Plastics*; Chiellini, E., Solaro, R., Eds.; Kluwer Academic/Plenum Publishers: New York, 2003. (e) *Poly(lactic acid): Synthesis, Structures, Properties, Processing, and Applications*; Auras, R., Lim, L.-T., Selke, S. E. M., Tsuji, H., Eds.; Wiley Series on Polymer Engineering and Technology; Wiley: Hoboken, NJ, 2010.

(2) (a) Santis, P. D.; Kovacs, A. J. *Biopolymers* **1968**, *6*, 299−306. (b) Hoogsteen, W.; Postema, A. R.; Pennings, A. J.; ten Brinke, G.; Zugenmaier, P. *Macromolecules* **1990**, *23*, 634−642. (c) Aleman, C.; Lotz, B.; Puiggali, J. *Macromolecules* **2000**, *34*, 4795−4801.

(3) (a) Sasaki, S.; Asakura, T. *Macromolecules* **2003**, *36*, 8385−8390. (b) Wasanasuk, K.; Tashiro, K.; Hanesaka, M.; Ohhara, T.; Kurihara, K.; Kuroki, R.; Tamada, T.; Ozeki, T.; Kanamoto, T. *Macromolecules* **2011**, *44*, 6441−6452.

(4) (a) Zhang, J.; Duan, Y.; Sato, H.; Tsuji, H.; Noda, I.; Yan, S.; Ozaki, Y. *Macromolecules* **2005**, *38*, 8012−8021. (b) Zhang, J.; Tashiro, K.; Domb, A. J.; Tsuji, H. *Macromol. Symp.* **2006**, *242*, 274−278. (c) Zhang, J.; Tashiro, K.; Tsuji, H.; Domb, A. J. *Macromolecules* **2008**, *41*, 1352−1357. (d) Cho, T. Y.; Strobl, G. *Polymer* **2006**, *47*, 1036−1043. (e) Kawai, T.; Rahman, N.; Matsuba, G.; Nishida, K.; Kanaya, T.; Nakano, M.; Okamoto, H.; Kawada, J.; Usuki, A.; Honma, N.; Nakajima, K.; Matsuda, M. *Macromolecules* **2007**, *40*, 9463−9469. (f) Pan, P.; Kai, W.; Zhu, B.; Dong, T.; Inoue, Y. *Macromolecules* **2007**, *40*, 6898−6905.

(5) (a) Wasanasuk, K.; Tashiro, K. *Polymer* **2011**, *52*, 6097−6109. (b) Wasanasuk, K.; Tashiro, K. *Macromolecules* **2011**, *44*, 9650−9660.

(6) (a) Marubayashi, H.; Akaishi, S.; Akasaka, S.; Asai, S.; Sumita, M. *Macromolecules* **2008**, *41*, 9192−9203. (b) Marubayashi, H.; Asai, S.; Sumita, M. *Polymer* **2012**, *53*, 4262−4271.

(7) (a) Eling, B.; Gogolewski, S.; Pennings, A. J. *Polymer* **1982**, *23*, 1587−1593. (b) Puiggali, J.; Ikada, Y.; Tsuji, H.; Cartier, L.; Okihara, T.; Lotz, B. *Polymer* **2000**, *41*, 8921−8930. (c) Sawai, D.; Takahashi, K.; Imamura, T.; Nakamura, K.; Kanamoto, T.; Hyon, S.-H. *J. Polym. Sci., Part B: Polym. Phys.* **2002**, *40*, 95−104. (d) Sawai, D.; Takahashi, K.; Sasashige, A.; Kanamoto, T.; Hyon, S.-H. *Macromolecules* **2003**, *36*, 3601−3605.

(8) Cartier, L.; Okihara, T.; Ikada, Y.; Tsuji, H.; Puiggali, J.; Lotz, B. *Polymer* **2000**, *41*, 8909−8919.

(9) Marubayashi, H.; Asai, S.; Sumita, M. *Macromolecules* **2012**, *45*, 1384−1397.

(10) Rizzo, P.; D'Aniello, C.; Del Mauro, A. D. G.; Guerra, G. *Macromolecules* **2007**, *40*, 9470−9474.

(11) Hashida, T.; Tashiro, K.; Ito, K.; Takata, M.; Sasaki, S.; Masunaga, H. *Macromolecules* **2010**, *43*, 402−408.

(12) Lai, W.-C. *J. Phys. Chem. B* **2011**, *115*, 11029−11037.

(13) Guerra, G.; Vitagliano, V. M.; De Rosa, C.; Petraccone, V.; Corradini, P. *Macromolecules* **1990**, *23*, 1539−1544.

(14) De Rosa, C.; Guerra, G.; Petraccone, V.; Pirozzi, B. *Macromolecules* **1997**, *30*, 4147−4152.

(15) Petraccone, V.; Ballesteros, D. R. O.; Tarallo, O.; Rizzo, P.; Guerra, G. *Chem. Mater.* **2008**, *20*, 3663−3668.

(16) Tarallo, O.; Schiavone, M. M.; Petraccone, V.; Daniel, C.; Rizzo, P.; Guerra, G. *Macromolecules* **2010**, *43*, 1455−1466.

(17) Uda, Y.; Kaneko, F.; Tanigaki, N.; Kawaguchi, T. *Adv. Mater.* **2005**, *17*, 1846−1850.

(18) (a) Rizzo, P.; Montefusco, T.; Guerra, G. *J. Am. Chem. Soc.* **2011**, *133*, 9872−9877. (b) Guerra, G.; Daniel, C.; Rizzo, P.; Tarallo, O. *J. Polym. Sci., Part B: Polym. Phys.* **2012**, *50*, 305−322.

(19) (a) Yoshioka, A.; Tashiro, K. *Macromolecules* **2003**, *36*, 3593−3600. (b) Tashiro, K.; Ueno, Y.; Yoshioka, A.; Kobayashi, M. *Macromolecules* **2001**, *34*, 310−315.

(20) Connolly, M. L. *J. Am. Chem. Soc.* **1985**, *107*, 1118−1124.

(21) (a) Senda, N. *Idemitsu Tech. Rep.* **2006**, *49*, 106−111. (b) Senda, N. Winmostar; http://winmostar.com/ (accessed 2012).

(22) Tamagawa, K.; Hilderbrandt, R. L.; Shen, Q. *J. Am. Chem. Soc.* **1987**, *109*, 1380−1383.

(23) Schultz, G.; Hargittai, I. *J. Phys. Chem.* **1993**, *97*, 4966−4969.

(24) Makarewicz, J.; Ha, T. K. *J. Mol. Struct.* **2001**, *599*, 271−278.

(25) Papoular, R. J.; Allouchi, H.; Chagnes, A.; Dzyabchenko, A.; Carre, B.; Lemordant, D.; Agafonov, V. *Acta Crystallogr., Sect. B: Struct. Sci.* **2005**, *61*, 312−320.

(26) Luger, P.; Buschmann, J. *Angew. Chem., Int. Ed. Engl.* **1983**, *22*, 410.
(27) (a) Hansen, C. M. *J. Paint Technol.* **1967**, *39*, 104−117. (b) Hansen, C. M.; Skaarup, K. *J. Paint Technol* **1967**, *39*, 511−514. (c) Koenhen, D. M.; Smolders, C. A. *J. Appl. Polym. Sci.* **1975**, *19*, 1163−1179. (d) Hansen, C. M. *Prog. Org. Coat.* **2004**, *51*, 55−66.
(28) Hansen, C. M. *Hansen Solubility Parameters: A User's Handbook*; CRC Press: Boca Raton, FL, 2000; pp 168−195.
(29) Agrawal, A.; Saran, A. D.; Rath, S. S.; Khanna, A. *Polymer* **2004**, *45*, 8603−8612.
(30) Stewart, J. J. P. *J. Mol. Model.* **2007**, *13*, 1173−1213.
(31) Simon, A.; Peters, K. *Acta Crystallogr.* **1980**, *B36*, 2750−2751.
(32) Kazarian, S. G.; Vincent, M. F.; Bright, F. V.; Liotta, C. L.; Eckert, C. A. *J. Am. Chem. Soc.* **1996**, *118*, 1729−1736.